

# Feasibility of carbon nanomaterials as gas sensors: a computational study

Deivasigamani Umadevi and G. Narahari Sastry\*

Centre for Molecular Modeling, CSIR–Indian Institute of Chemical Technology, Hyderabad 500 607, India

Carbonaceous materials are a promising class of materials for potential application as chemical and biomolecule sensors. In this work we have done first principles calculations to study the interaction of various small molecules, such as CO<sub>2</sub>, H<sub>2</sub>O, NH<sub>3</sub>, CH<sub>4</sub> and H<sub>2</sub>, on the surface of carbon nanotubes (CNTs) and graphene in order to study their feasibility as gas sensors. Model systems for armchair and zigzag CNTs of different diameter have been considered to study the effect of chirality and curvature of the carbon nanomaterials on binding with these small molecules. Our results reveal that these gas molecules have been weakly physisorbed on the surface and act as charge donors to the carbon nanomaterials. Charge transfer between the gas molecules and the carbon materials impacts the physical properties of the carbon materials, which may be traced to their sensitivity. As the gas molecules are physisorbed on the carbon materials, they may be suitable for repetitive sensor operation. Significant changes in the polarizability of the carbon materials have been observed on binding with the gas molecules and monitoring such changes provides valuable guidance in designing optimal gas sensors based on carbon materials that could satisfy the demand in various fields.

**Keywords:** Gas sensors, graphene, modeling nanoparticles, nanotube, noncovalent interaction.

## Introduction

THE topical carbon allotropes graphene and carbon nanotubes (CNTs) have gained significant research interest due to their unique properties and potential applications. The exceptional electronic, thermal, optical, mechanical and transport properties of these carbon materials make them promising candidates for various potential applications<sup>1–3</sup>. It has been observed from several experimental and theoretical studies that the transport and electronic properties of the carbon materials are extremely sensitive to changes in the local chemical environment<sup>4–6</sup>. This inference paved the way for the progress of carbon nanomaterials-based gas sensors. Development of chemical and biological sensors based on carbon nanomaterials is

an area of recent interest<sup>7,8</sup>. Gas sensing materials have gained considerable research interest due to their widespread applications in various sectors such as energy and environment, homeland security and as chemical warfare agents<sup>9–11</sup>. Recent experimental studies have shown that reduced graphene oxide exhibits superior gas sensing properties<sup>12–14</sup>. There is immense demand for highly sensitive gas sensors to detect explosive and poisonous gas leakages in various chemical and pharmaceutical industries. The advancement in the carbon-based nanotechnology has enhanced the possibility of low-cost and highly sensitive sensors for various applications<sup>15</sup>.

The structure and physical properties of carbon nanostructures (CNS) make them potential candidates as sensors to detect different gases. Dai and co-workers were the first to report the gas sensors based on CNTs to detect gases such as NO<sub>2</sub> and NH<sub>3</sub> (ref. 16). A recent experimental study stated that graphene-based sensors possess very high sensitivity such that the adsorption of individual gas molecules could be detected<sup>17</sup>. In general, the principle of gas sensing involves adsorption and desorption of gas molecules on the sensing materials. The extremely high surface-to-volume ratio and hollow structure of nanomaterials are ideal for the adsorption of gas molecules. The adsorption of various substrates such as metal ions, gas molecules, drug molecules, organic molecules and biomolecules such as proteins and nucleic acids on the surface of the carbon materials has gained significant interest because of their fundamental importance and potential industrial applications<sup>18–23</sup>. Derouane and co-workers have studied the effect of the surface curvature on the physisorption binding energies<sup>24–26</sup>. If the substrates thus adsorbed are capable of modifying the electronic and magnetic properties of the carbon materials, then by monitoring such specific changes the presence of different species can be detected. Selective detection of gas molecules based on the change in dielectric constant of CNTs has been studied<sup>27</sup>. Meyyappan and co-workers developed a CNT sensor platform for gas and organic vapour detection at room temperature and explained the molecular sensing in terms of charge transfer mechanism<sup>28</sup>. Mirica *et al.*<sup>29</sup> developed a solvent-free approach for fabricating CNT gas sensors on the surface of cellulosic paper by mechanical abrasion. Besides, hybrid carbon nanomaterials have also been found to show promising gas sensing abilities<sup>30,31</sup>.

\*For correspondence. (e-mail: gnsastry@gmail.com)

The adsorption/desorption mechanism will be more effective if the substrate molecules are weakly bound on the surface of the carbon nanostructures. Hence a noncovalent type of interaction is preferred to covalent binding, where there is a bond formation and bond breaking. Understanding the noncovalent interactions on the surfaces of carbon materials is important to get fundamental and molecular level understanding about their various applications<sup>32–36</sup>. Factors influencing the noncovalent interactions such as size and curvature of the  $\pi$ -system have been studied extensively<sup>37–41</sup>. Graphene is a two-dimensional sheet of  $sp^2$  carbon atoms and CNTs are the wrapped-up graphene sheets in one dimension<sup>42</sup>. It is interesting to compare and contrast the reactivity of these two allotropes which vary in their curvature towards various species<sup>43–47</sup>. Besides, CNTs can be classified into different types such as armchair, zigzag and chiral nanotubes based on the orientation of the tube axis with respect to the hexagonal lattice<sup>48</sup>. It has been shown in the literature that functionalization of the carbon nano-materials would enhance the adsorption of various species<sup>49,50</sup>. The covalent and noncovalent functionalization of graphene has been studied in a recent review<sup>51</sup>. Apart from the traditional CNTs, the inorganic nanotubes have also been shown to have promising potential for sensor applications<sup>52,53</sup>.

The present study aims to provide a comprehensive and comparative analysis of the noncovalent interaction of various gas molecules such as  $CO_2$ ,  $H_2O$ ,  $CH_4$ ,  $NH_3$  and  $H_2$  with CNTs of varying diameter and chirality and graphene nano ribbons (GNRs). The orientations of these gas molecules on the surface of the CNS and their binding strength have been estimated. The effect of curvature and chirality of the carbon materials on the binding strength has been studied. The charge transfer that occurred during the complex formation has also been explored. The change in the polarizability of CNS upon the binding of these gas molecules has been estimated.

## Computational methods and model systems

The geometry of all the structures considered was optimized using two-layer ONIOM calculations at (M06–2X/6–31G\*: AM1) level of theory, in which a seven-ring fragment resembling coronene is considered as high layer and the rest of the system is considered as low layer (Figure 1). The geometries were optimized using Berny optimization and the convergence criteria. Though many popular functionals fail to describe the noncovalent interactions, the *de novo* parameterized M06-2X functionals developed by Zhao and Truhlar<sup>54</sup> have been shown to give good performance for the noncovalent interactions. All stationary points were characterized as minima after verifying the presence of all real frequencies. Although basis set superposition error (BSSE) correction is impor-

tant for noncovalent interactions<sup>55–57</sup>, it has been found that for density functional theory (DFT) methods there is no significant change in the results<sup>58,59</sup>. Hence we have not employed BSSE corrections in the present study.

To test the reliability of our ONIOM approach for accurate description for geometric parameters, we have also done full geometry optimization at M06-2X/6-31G\* level for the CNT (4,4) complexes. In Table 1, the binding energy (BE) and geometric parameters of the full systems have been compared with the ONIOM results. A quick look at Table 1 shows that the results obtained in the ONIOM approach are in good agreement with the full system optimization. Subsequently, we have made the single-point calculation using M06-2X/6-311G\*\* level of theory for the complete system of the optimized structures. The binding energy was calculated by the super-molecule approach using eq. (1) as the difference between sum of the total energies of the parent CNS ( $E_{CNS}$ ) and the gas molecules ( $E_X$ ) (where  $X = CO_2, H_2O, NH_3, CH_4$  and  $H_2$ ) and the total energy of the complex ( $E_{CNS-X}$ ).

$$BE = (E_{CNS} + E_X) - E_{CNS-X} \quad (1)$$

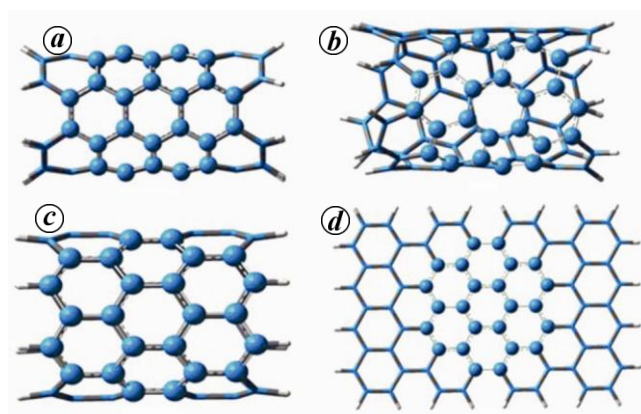
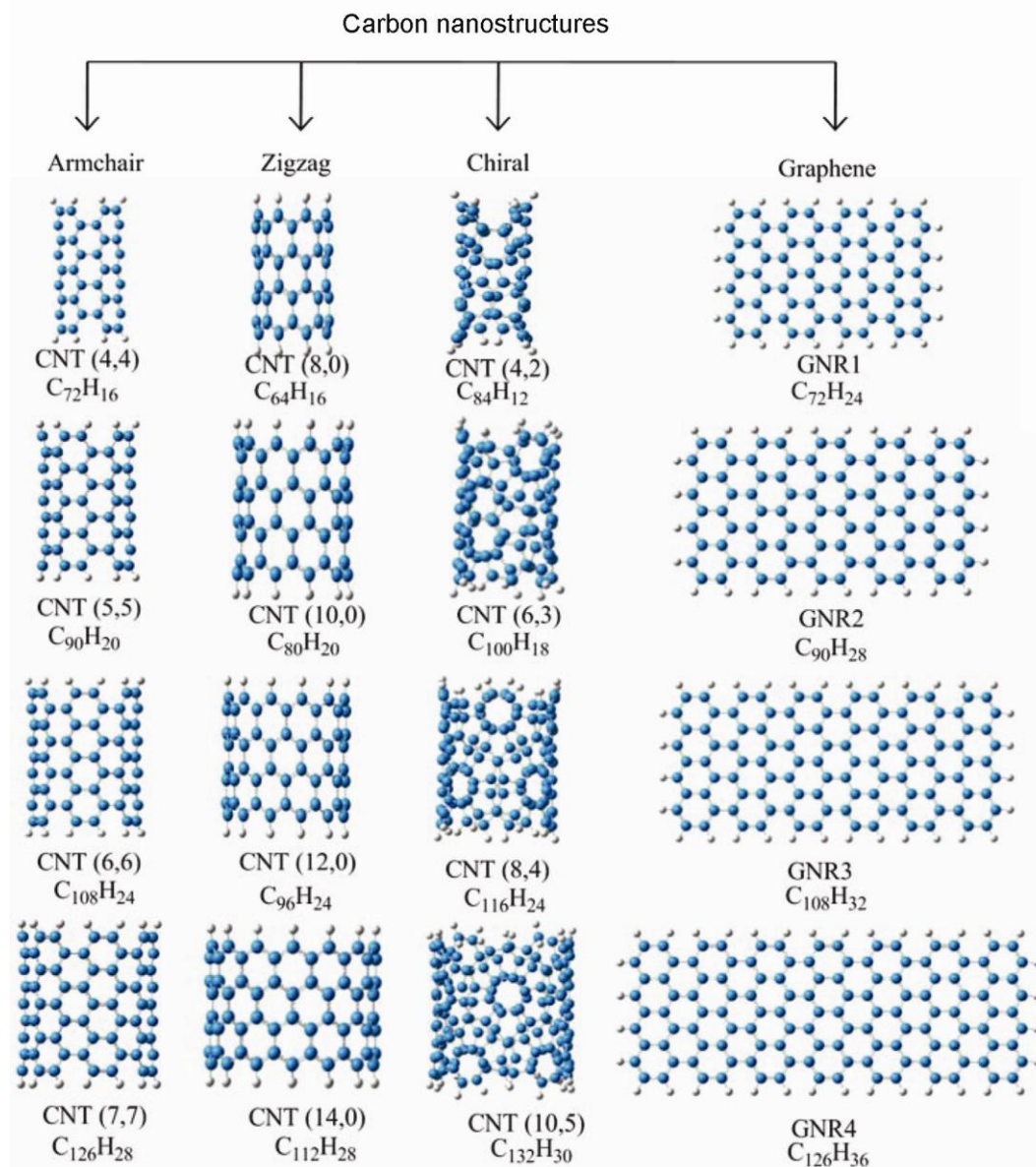


**Figure 1.** Atoms shown by ball and bond model considered for high layer and the rest of the atoms shown by tube model considered for low layer in the ONIOM calculation. *a*, Armchair CNT; *b*, chiral CNT; *c*, zigzag CNT; *d*, graphene nano ribbons (GNRs).

**Table 1.** Binding energy (BE) (kcal/mol) and distance (Å) of the gas molecules with carbon nanotube (CNT) (4,4) obtained using ONIOM approach and full optimization

Molecule	M06-2X/6-31G*//ONIOM (M06-2X/6-31G*: AM1)		M06-2X/6-31G*	
	BE	<i>d</i>	BE	<i>d</i>
$CO_2$	4.07	2.987	4.07	2.956
$H_2O$	4.35	2.522	4.33	2.501
$CH_4$	2.26	2.892	2.27	2.856
$NH_3$	3.63	2.733	3.61	2.748
$H_2$	1.13	2.677	1.13	2.683



**Scheme 1.** Nomenclature and molecular formula of the model systems considered for carbon nanostructures.

Polarizability is considered to be a measure of the potential of a molecule to respond to an external electric field. When a molecule is subjected to an external electric field, some of its electrons obtain adequate energy to move along the direction of the electric field. The average molecular polarizability ( $\bar{\alpha}$ ) was calculated as the average of the diagonal components of the polarizability tensor as shown in eq. (2).

$$\bar{\alpha} = (\alpha_{xx} + \alpha_{yy} + \alpha_{zz})/3, \quad (2)$$

where  $\alpha_{xx}$ ,  $\alpha_{yy}$  and  $\alpha_{zz}$  are the diagonal components of the polarizability tensor calculated at M06-2X/6-31G\* level. All the calculations were done in Gaussian 09 suite of program<sup>60</sup>.

We have considered a wide range of model systems to represent the CNTs and graphene as shown in Scheme 1. A set of armchair CNTs such as CNT(4,4), CNT(5,5), CNT(6,6), CNT(7,7) and a set of zigzag CNTs such as CNT(8,0), CNT(10,0), CNT(12,0), CNT(14,0) have been modeled (Table S1; [see Supporting information online](#)). In addition, we have generated models for chiral CNTs such as CNT(4,2), CNT(6,3), CNT(8,4) and CNT(10,5). The eclectic model systems considered will help determine the effect of chirality of CNTs on binding with the gas molecules. Further, in order to study the effect of curvature on binding energy, we have considered graphene nano ribbons GNR1, GNR2, GNR3 and GNR4, which were the opened flat models of the nanotubes CNT(4,4), CNT(5,5), CNT(6,6) and CNT(7,7) respectively. The binding of

**Table 2.** Distance (Å) between gas molecules and carbon nanostructures (CNS) in the optimized geometry at ONIOM (M06-2X/6-31G\*: AM1) level of theory

CNS		Distance (Å)				
	No. of atoms	CO <sub>2</sub>	H <sub>2</sub> O	CH <sub>4</sub>	NH <sub>3</sub>	H <sub>2</sub>
<b>Armchair</b>						
CNT (4,4)	88	2.987	2.522	2.892	2.733	2.677
CNT (5,5)	110	2.995	2.584	2.753	2.772	2.666
CNT (6,6)	132	3.030	2.578	2.783	2.797	2.668
CNT (7,7)	154	3.018	2.607	2.738	2.825	2.686
<b>Zigzag</b>						
CNT (8,0)	80	2.966	2.732	2.149	2.901	2.825
CNT (10,0)	100	2.961	2.731	2.803	2.878	2.777
CNT (12,0)	120	2.981	2.706	2.425	2.811	2.756
CNT (14,0)	140	2.966	2.704	2.495	2.867	2.754
<b>Chiral</b>						
CNT (4,2)	96	2.994	2.461	2.515	2.741	2.693
CNT (6,3)	118	2.985	2.510	2.646	2.765	2.663
CNT (8,4)	140	3.002	2.556	2.684	2.796	2.674
CNT (10,5)	162	3.013	2.615	2.721	2.808	2.663
<b>Graphene</b>						
GNR1	96	3.028	2.650	2.790	2.861	2.693
GNR2	118	3.029	2.649	2.791	2.787	2.688
GNR3	140	3.030	2.658	2.787	2.868	2.698
GNR4	162	2.995	2.663	2.807	2.819	2.679

various gas molecules such as CO<sub>2</sub>, H<sub>2</sub>O, CH<sub>4</sub>, NH<sub>3</sub> and H<sub>2</sub> on these CNS have been studied.

## Results and discussion

In this section, at the outset we discuss the orientation of the gas molecules on the CNS surface in the optimized structure as well as the changes in their geometric parameters upon complex formation. Subsequently, we look at the binding energy of the carbon nanostructures with various gas molecules and the trend in the charge transfer. The change in the characteristic vibration frequency of these gas molecules on binding with the CNS has been analysed. This is followed by a discussion on the polarizability and HOMO–LUMO energy gap of the CNS complexes.

## Structure and geometry

We have considered various possible orientations of these gas molecules on the surface of the CNS and reported only the minimum energy orientations. The nearest distance (*d*) between the surface of the CNS and the gas molecules has been measured and given in Table 2 for all the complexes considered. The *d* values given in Table 2 represent the distance from the surface of the CNS to the nearest H atom in the gas molecules, except in the case of CO<sub>2</sub> where the *d* value represents the distance between

the surface of the CNS and the C atom of the CO<sub>2</sub> molecule.

The CO<sub>2</sub> molecule has been observed to have a parallel mode of orientation above the surface of the CNS in the optimized structures. The C atom of the CO<sub>2</sub> molecule is just above the C–C double bond at a distance of around 2.961–3.030 Å, as shown in Figure 2. The H<sub>2</sub>O molecule is oriented above the CNS surface such that the two OH groups are pointing towards the surface. The distance between the H atom and the surface of the CNS has been found to be in the range 2.461–2.732 Å. In the minimum energy orientation of the NH<sub>3</sub> complexes, all the three N–H groups are pointing towards the surface of the carbon nanostructures, whereas in the case of CH<sub>4</sub>, three C–H bonds are oriented towards the CNS surface and the fourth C–H bond is away from the surface (Figure 2). From the surface of the CNS, the nearest distance between the NH<sub>3</sub> molecule ranges between 2.733 and 2.901 Å, whereas the distance of the CH<sub>4</sub> molecule ranges between 2.149 and 2.892 Å. The H<sub>2</sub> molecule oriented itself perpendicular to the surface of the CNS at distances around 2.666–2.825 Å.

The geometric parameters of the gas molecules before and after complex formation are given in Table 3. In the case of CO<sub>2</sub>, the C–O bond length in its free state is 1.163 Å on both sides. Table 3 reveals that in the CNS–CO<sub>2</sub> complexes, there is a slight increase in the bond length of one of the C–O bonds. For H<sub>2</sub>O, the O–H distance in the molecule is 0.965 Å, whereas in the

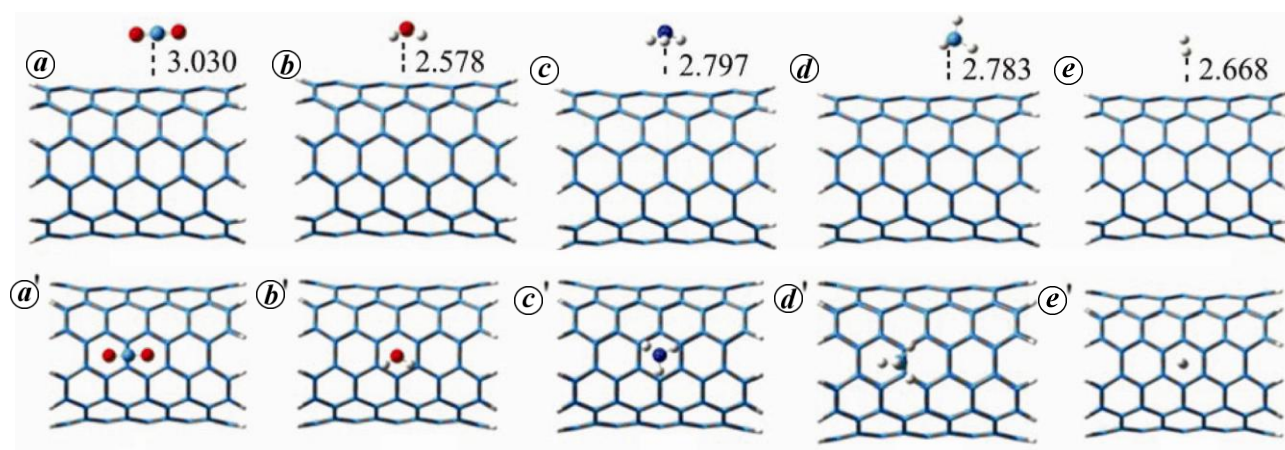


**Figure 2.** A representative case to show the mode of interaction and distance ( $\text{\AA}$ ) of (a, a')  $\text{CO}_2$ , (b, b')  $\text{H}_2\text{O}$ , (c, c')  $\text{NH}_3$ , (d, d')  $\text{CH}_4$  and (e, e')  $\text{H}_2$  with  $\text{CNT}(6,6)$ . The side and front views are given in the first and second rows respectively. All other carbon materials follow the same mode of interaction with the gas molecules.

**Table 3.** Geometric parameters ( $\text{\AA}$ ) of the gas molecules before and after complexation with CNS at ONIOM (M06-2X/6-31G\*: AM1) level of theory

	$\text{CO}_2$		$\text{H}_2\text{O}$		$\text{CH}_4$				$\text{NH}_3$			$\text{H}_2$
	C-O (1)	C-O (2)	O-H (1)	O-H (2)	C-H (1)	C-H (2)	C-H (3)	C-H (4)	N-H (1)	N-H (2)	N-H (3)	H-H
Free state	1.163	1.163	0.965	0.965	1.092	1.092	1.092	1.092	1.017	1.017	1.017	0.736
<b>Armchair</b>												
CNT (4,4)	1.163	1.164	0.967	0.967	1.092	1.092	1.092	1.092	1.018	1.018	1.018	0.739
CNT (5,5)	1.163	1.164	0.966	0.966	1.092	1.092	1.092	1.093	1.018	1.018	1.018	0.739
CNT (6,6)	1.163	1.164	0.966	0.966	1.092	1.092	1.092	1.093	1.018	1.018	1.018	0.739
CNT (7,7)	1.163	1.164	0.966	0.966	1.092	1.092	1.092	1.093	1.018	1.018	1.018	0.738
<b>Zigzag</b>												
CNT (8,0)	1.163	1.164	0.967	0.967	1.092	1.092	1.092	1.092	1.017	1.018	1.018	0.738
CNT (10,0)	1.162	1.165	0.967	0.967	1.092	1.092	1.092	1.093	1.018	1.018	1.018	0.739
CNT (12,0)	1.163	1.163	0.967	0.967	1.092	1.092	1.092	1.093	1.018	1.018	1.018	0.738
CNT (14,0)	1.163	1.164	0.967	0.967	1.092	1.092	1.092	1.093	1.018	1.018	1.018	0.738
<b>Chiral</b>												
CNT (4,2)	1.163	1.163	0.967	0.967	1.092	1.092	1.092	1.092	1.018	1.018	1.018	0.738
CNT (6,3)	1.163	1.164	0.966	0.967	1.092	1.092	1.092	1.093	1.018	1.018	1.018	0.739
CNT (8,4)	1.163	1.164	0.966	0.966	1.092	1.092	1.092	1.093	1.018	1.018	1.018	0.738
CNT (10,5)	1.163	1.164	0.966	0.966	1.092	1.092	1.092	1.093	1.018	1.018	1.018	0.738
<b>Graphene</b>												
GNR1	1.163	1.164	0.967	0.967	1.092	1.092	1.093	1.093	1.018	1.018	1.018	0.739
GNR2	1.163	1.164	0.967	0.967	1.092	1.092	1.093	1.093	1.018	1.018	1.018	0.739
GNR3	1.163	1.164	0.967	0.967	1.092	1.092	1.093	1.093	1.018	1.018	1.018	0.739
GNR4	1.163	1.164	0.967	0.967	1.092	1.092	1.093	1.093	1.018	1.018	1.018	0.738

complexed state the O–H bond length increases up to 0.967  $\text{\AA}$ . The C–H bond length in the  $\text{CH}_4$  molecule is 1.092  $\text{\AA}$  when it is in the unbound state. While three of the C–H bond lengths remain the same on binding with the CNS, the fourth C–H bond pointing towards the CNS in the optimized geometry shows a slight increase in bond length. In the unbound state the N–H bond length in  $\text{NH}_3$  is 1.017  $\text{\AA}$ ; however, all the three N–H bond lengths become 1.018  $\text{\AA}$  on binding with the CNS. For  $\text{H}_2$  mole-

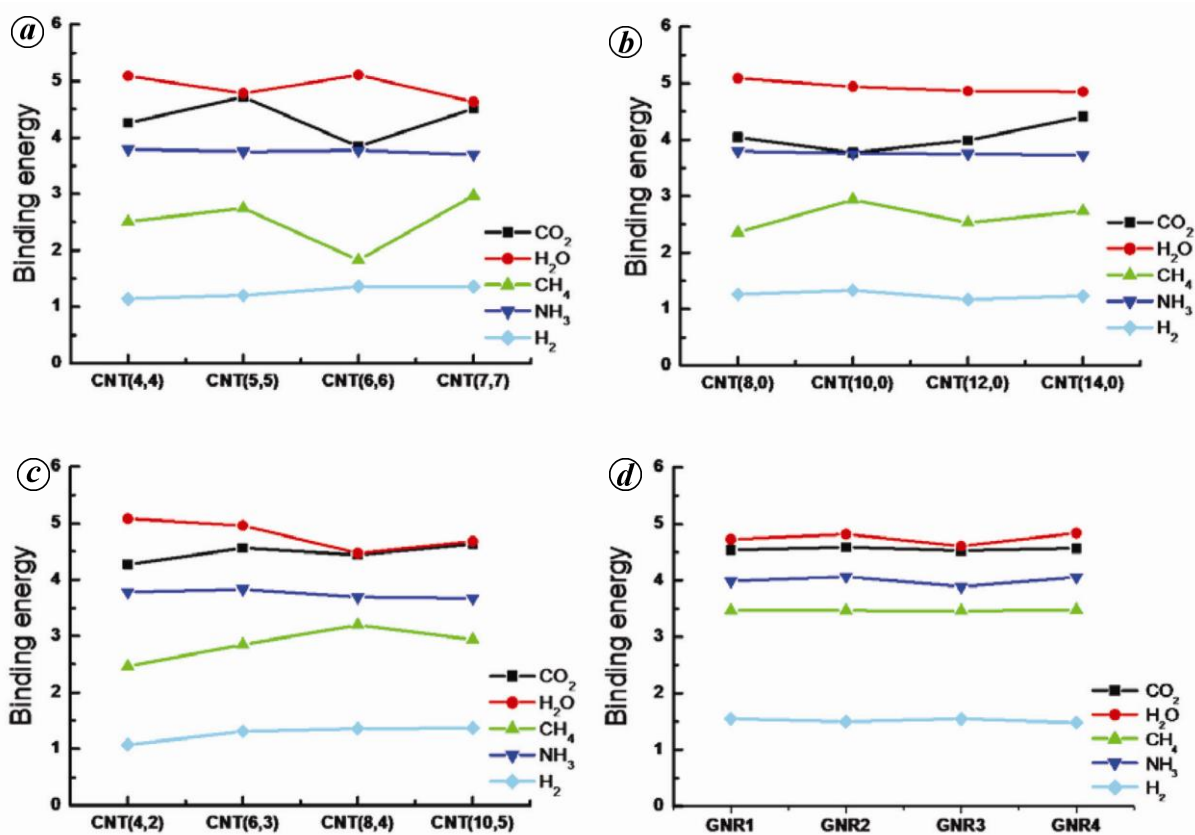
cule, the H–H bond distance is 0.736  $\text{\AA}$  in the unbound state and it increased up to 0.739  $\text{\AA}$  while binding with CNS.

### Binding energy and charge transfer

We further calculated the binding energy of all the molecules considered with CNS at M06-2X/6-311G\*\* level. Table 4 shows the binding energy of the gas molecules

**Table 4.** BE (kcal/mol) of CNS with gas molecules at M06-2X/6-311G\*\*//ONIOM(M06-2X/6-31G\*: AM1) level of theory

CNS		BE (kcal/mol)				
No. of atoms		CO <sub>2</sub>	H <sub>2</sub> O	CH <sub>4</sub>	NH <sub>3</sub>	H <sub>2</sub>
<b>Armchair</b>						
CNT (4,4)	88	4.26	5.09	2.51	3.79	1.14
CNT (5,5)	110	4.72	4.78	2.75	3.75	1.20
CNT (6,6)	132	3.84	5.11	1.83	3.77	1.36
CNT (7,7)	154	4.51	4.63	2.97	3.70	1.36
<b>Zigzag</b>						
CNT (8,0)	80	4.04	5.09	2.36	3.80	1.26
CNT (10,0)	100	3.77	4.94	2.94	3.76	1.33
CNT (12,0)	120	3.99	4.86	2.53	3.75	1.17
CNT (14,0)	140	4.41	4.85	2.74	3.73	1.23
<b>Chiral</b>						
CNT (4,2)	96	4.27	5.08	2.46	3.78	1.07
CNT (6,3)	118	4.56	4.96	2.85	3.83	1.31
CNT (8,4)	140	4.44	4.47	3.20	3.69	1.36
CNT (10,5)	162	4.63	4.68	2.94	3.67	1.37
<b>Graphene</b>						
GNR1	96	4.54	4.73	3.47	3.99	1.55
GNR2	118	4.59	4.82	3.47	4.07	1.50
GNR3	140	4.53	4.61	3.46	3.89	1.55
GNR4	162	4.57	4.84	3.48	4.06	1.48


**Figure 3.** Binding energy (kcal/mol) of the gas molecules CO<sub>2</sub>, H<sub>2</sub>O, CH<sub>4</sub>, NH<sub>3</sub> with (a) armchair CNTs, (b) zigzag CNTs, (c) chiral CNTs and (d) GNRs at M06-2X/6-311G\*\*//ONIOM (M06-2X/6-31G\*: AM1) level of theory.

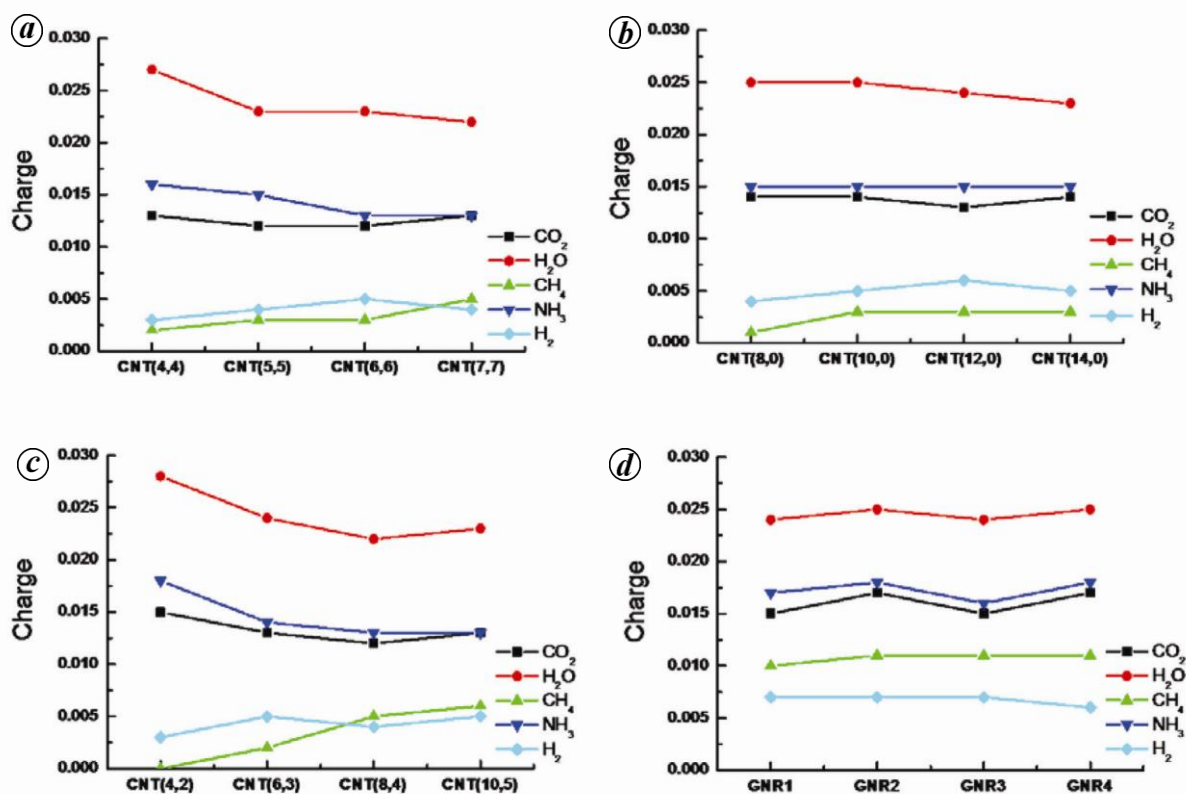


**Figure 4.** Mulliken charge (amu) on the gas molecules in their complex form with (a) armchair CNTs, (b) zigzag CNTs, (c) chiral CNTs and (d) GNRs at M06-2X/6-311G\*\*/ONIOM (M06-2X/6-31G\*: AM1) level of theory.

with armchair CNTs, zigzag CNTs, chiral CNTs and GNRs. It can be surmised from the table that these molecules have been weakly adsorbed on the surface of the carbon materials with very less binding energy of about  $\sim 5$  kcal/mol. In general, the order of magnitude of binding energy for the physisorption process is considered to be less than 5 kcal/mol and the aforesaid energy for chemisorption is usually higher than 15 kcal/mol. Our numerical study connotes that these gas molecules interact with CNTs and graphene by physisorption and so the desorption phenomenon will be easier. Such an adsorption/desorption mechanism is an important prerequisite for various sensor materials for repeatable sensor operation. A closer glance at the binding energy of the gas molecules with different CNTs (armchair, zigzag and chiral) indicates that there is no substantial effect of chirality on the binding energy, in contrast to our earlier observations on cation- $\pi$  and  $\pi$ - $\pi$  interactions with the carbon nanostructures. This can be attributed to the very weak interactions between these gas molecules and CNTs. The effect of curvature of the carbon materials on binding with various species is a topic of interest. Graphene is a two-dimensional sheet of carbon and CNTs are wrapped graphene in one dimension. Hence comparing the properties of flat graphene with that of the curved CNTs is interesting. Our results show that graphene exhibits marginally higher binding energy than the corre-

sponding CNTs in most cases. The order of binding energy of these gas molecules on the surface of the CNS is as  $\text{H}_2\text{O} > \text{CO}_2 > \text{NH}_3 > \text{CH}_4 > \text{H}_2$  (Figure 3).

In order to gauge the mechanism of these foregoing binding interactions, we have done the Mulliken charge analysis at M06-2X/6-311G\*\* level (Figure 4 and Table S2; [see Supporting information online](#)). Charge transfer is a phenomenon in which a large fraction of an electronic charge is transferred from one molecular entity (charge donor) to another (charge acceptor). As a result of the charge transfer electronic structure of the sensor materials will be affected, thus leading to changes in their electronic properties. The positive charge values on the gas molecules in the optimized complexes clearly point out that these gas molecules act as charge donors to the carbon nanostructures. The highest charge transfer has occurred in the case of H<sub>2</sub>O molecule. The neutral H<sub>2</sub>O molecules obtained a partial positive charge of about 0.28 amu on binding with different CNS. The amount of charge transfer that occurred in the case of CO<sub>2</sub> and NH<sub>3</sub> has been found to be very close in magnitude. The H<sub>2</sub> molecule exhibits the slightest charge transfer in most of the cases, except in a few cases where the CH<sub>4</sub> molecule shows the least charge transfer, as shown in Figure 4. In line with the observation in the case of binding energy, the extent of charge transfer from the gas molecule to CNTs is independent of the type and chirality of CNTs,

**Table 5.** Characteristic stretching and bending frequencies ( $\text{cm}^{-1}$ ) of gas molecules before and after complex formation with CNS

	CO <sub>2</sub> $\delta_{\text{C-O}}$	CO <sub>2</sub> $\nu_{\text{C-O}}$	CO <sub>2</sub> $\nu_{\text{C-O}}$	H <sub>2</sub> O $\delta_{\text{O-H}}$	H <sub>2</sub> O $\nu_{\text{O-H}}$	H <sub>2</sub> O $\nu_{\text{O-H}}$	CH <sub>4</sub> $\delta_{\text{C-H}}$	CH <sub>4</sub> $\delta_{\text{C-H}}$	CH <sub>4</sub> $\nu_{\text{C-H}}$	CH <sub>4</sub> $\nu_{\text{C-H}}$	NH <sub>3</sub> $\delta_{\text{N-H}}$	NH <sub>3</sub> $\delta_{\text{N-H}}$	NH <sub>3</sub> $\nu_{\text{N-H}}$	NH <sub>3</sub> $\nu_{\text{N-H}}$	H <sub>2</sub> $\nu_{\text{H-H}}$
Isolated	668	1421	2499	1706	3814	3934	1381	1603	3087	3210	1138	1726	3485	3620	4523
CNT (4,4)	647	1416	2479	1706	3803	3916	1363	1596	3073	3200	1159	1724	3473	3606	4550
CNT (5,5)	647	1417	2480	1702	3800	3915	1370	1598	3078	3203	1150	1721	3478	3610	4555
CNT (6,6)	648	1417	2477	1702	3802	3917	1366	1595	3080	3203	1153	1722	3474	3606	4555
CNT (7,7)	651	1417	2478	1703	3801	3916	1382	1597	3072	3193	1157	1725	3480	3610	4532
CNT (8,0)	644	1418	2481	1705	3808	3920	1374	1594	3079	3200	1155	1723	3476	3611	4531
CNT (10,0)	645	1416	2476	1706	3802	3915	1371	1594	3077	3202	1153	1721	3476	3606	4554
CNT (12,0)	646	1418	2472	1702	3809	3922	1371	1598	3078	3205	1161	1720	3477	3608	4565
CNT (14,0)	646	1415	2471	1704	380	3921	1370	1598	3078	3205	1157	1724	3480	3612	4541
CNT (4,2)	643	1416	2477	1705	3806	3916	1375	1596	3077	3199	1160	1720	3477	3608	4563
CNT (6,3)	645	1416	2477	1702	3808	3921	1375	1598	3081	3203	1153	1725	3478	3609	4545
CNT (8,4)	649	1416	2477	1703	3802	3916	1372	1592	3071	3192	1153	1720	3477	3610	4534
CNT (10,5)	647	1419	2483	1705	3811	3923	1378	1592	3073	3193	1171	1720	3482	3614	4528
GNR1	654	1417	2479	1705	3797	3911	1377	1593	3069	3193	1165	1720	3476	3606	4552
GNR2	651	1417	2478	1709	3805	3920	1376	1593	3068	3192	1170	1723	3474	3605	4553
GNR3	654	1417	2479	1705	3798	3913	1368	1593	3069	3194	1166	1721	3477	3606	4554
GNR4	651	1417	2479	1708	3804	3918	1368	1593	3068	3192	1163	1723	3469	3609	4527

whereas charge transfer is more in the case of flat graphene compared to the curved CNTs.

### Vibrational analysis

Spectroscopic signatures will be of immense importance in experimentally validating the computational predictions. The shifts in the characteristic vibration frequencies of the gas molecules upon complex formation with various carbon nanostructures have been computed at ONIOM (M06-2X/6-31G\*: AM1) level. The frequencies reported in Table 5 have not been scaled by any factor. For an isolated CO<sub>2</sub> molecule, there exist three characteristic vibrations, namely  $\nu_1 = 668 \text{ cm}^{-1}$ ,  $\nu_2 = 1421 \text{ cm}^{-1}$  and  $\nu_3 = 2499 \text{ cm}^{-1}$ , which correspond to the bending, symmetric and asymmetric stretching modes of C–O bond respectively. A brief glance at the table shows that all the three CO<sub>2</sub> characteristic vibrations decrease upon binding with the carbon materials, which indicates a red shift.

Next, we look at the case of the H<sub>2</sub>O molecule. There are three characteristic vibrational modes, namely  $\nu_1 = 1706 \text{ cm}^{-1}$ ,  $\nu_2 = 3814 \text{ cm}^{-1}$  and  $\nu_3 = 3934 \text{ cm}^{-1}$ , which correspond to O–H bending and stretching. Our results indicate that in CNS–H<sub>2</sub>O complexes, the O–H stretching frequencies depict a smaller red shift. For CH<sub>4</sub> molecule there are two C–H stretching and two bending modes observed for the free molecule. It is clear from Table 5 that these frequencies show a red shift on binding with the carbon materials. In the case of NH<sub>3</sub> molecule, while the N–H bending frequency shows a blue shift, the rest of the vibrational modes shows a red shift upon binding with the CNS. The characteristic vibration mode of the

H<sub>2</sub> molecule which arises due to the H–H stretching at  $4523 \text{ cm}^{-1}$  in the free molecule exhibits a blue shift on binding with the carbon materials.

### Polarizability and frontier orbital energy

The primary requisite for a material to perform as a sensor is to undergo a change in its physical property on interacting with an analyte. Such changes can be monitored and recorded to determine the presence of the analyte. In order to notice such depiction in the case of carbon materials, we have calculated the polarizability and frontier orbital energy of the carbon materials both in the free state and in the complexed state. Polarizability is considered to be the ability of a molecule to respond to an external electric field. The molecular polarizability of all the systems considered have been computed and given in Table 6. A cursory look at the table reveals that the flat graphene has higher polarizability than the curved CNTs. This observed trend explains the higher binding affinity of graphene compared to CNTs. Among the CNTs, zigzag CNTs possess the highest polarizability compared to the armchair and chiral counterparts. If we compare the parent system with that of the complexes, there is an increase in the polarizability of the carbon materials on binding with the gas molecules (Table S3; see [Supporting information online](#)). The change observed in the polarizability is found to be maximum in the case of CH<sub>4</sub> complexes. The next significant change has been observed in the case of CO<sub>2</sub> complexes, followed by NH<sub>3</sub> and H<sub>2</sub>O respectively. The complexes with the H<sub>2</sub> molecule show the least change in the polarizability value

**Table 6.** Polarizability (au) of CNS and CNS–gas molecule complexes at M06-2X/6-31G\* level

	Pristine	CO <sub>2</sub>	H <sub>2</sub> O	CH <sub>4</sub>	NH <sub>3</sub>	H <sub>2</sub>
<b>Armchair</b>						
CNT (4,4)	727.82	739.28	733.98	740.87	736.70	732.60
CNT (5,5)	970.65	982.50	976.87	984.32	979.64	975.87
CNT (6,6)	1196.33	1208.28	1202.84	1210.20	1205.26	1201.45
CNT (7,7)	1466.85	1478.87	1473.49	1480.85	1475.91	1471.50
<b>Zigzag</b>						
CNT (8,0)	942.10	952.62	949.64	954.66	951.32	948.27
CNT (10,0)	1235.52	1247.42	1242.83	1249.32	1244.54	1241.02
CNT (12,0)	1490.15	1501.59	1501.63	1503.82	1499.13	1495.45
CNT (14,0)	1779.35	1796.31	1797.54	1793.23	1788.39	1782.33
<b>Chiral</b>						
CNT (4,2)	569.29	578.91	574.68	582.05	577.56	573.69
CNT (6,3)	841.53	853.37	847.93	855.53	850.64	846.61
CNT (8,4)	1307.38	1319.70	1314.16	1322.09	1316.19	1312.25
CNT (10,5)	1826.61	1838.38	1833.05	1840.60	1835.41	1831.18
<b>Graphene</b>						
GNR1	1862.88	1869.68	1865.38	1870.42	1866.36	1865.75
GNR2	2870.89	2877.31	2873.78	2875.63	2874.89	2873.73
GNR3	4071.56	4077.99	4074.54	4078.55	4075.42	4072.62
GNR4	5538.41	5544.43	5527.26	5543.98	5542.21	5541.22

compared to the other molecules considered. Because polarizability has an effect on the electronic response of the system, change in polarizability may be used to monitor the presence of gas molecules. We have also calculated the HOMO–LUMO energy gap (Table S4; see [Supporting information online](#)) of the carbon materials and their complexes. It has been shown from our computations that the energy gap for graphene is lower than the CNTs. Zigzag CNTs possess the lowest energy gap among the CNTs considered. Notably, there is no significant change in the HOMO–LUMO energy gap of the carbon materials upon binding with the gas molecules.

## Conclusions

In this study, to investigate the feasibility of carbon materials as gas sensors, we have studied the interaction of various gas molecules such as CO<sub>2</sub>, H<sub>2</sub>O, CH<sub>4</sub>, NH<sub>3</sub> and H<sub>2</sub> with CNTs and graphene using DFT calculations. It can be seen from our results that the order of binding of these gas molecules is H<sub>2</sub>O > CO<sub>2</sub> > NH<sub>3</sub> > CH<sub>4</sub> > H<sub>2</sub>.

We have found that the flat graphene exhibits marginally strong binding energy than the curved CNTs. These molecules are very weakly physisorbed on the surface of the CNS and the binding energy is independent of the type of carbon material. The weak adsorption of the gas molecules facilitates the adsorption/desorption mechanism, which is a primary requirement for sensor process. The Mulliken charge analysis reveals that these gas molecules act as charge donors to the carbon nanostructures

and influence the physical properties of the carbon materials, which leads to the sensitivity. The shifts in the vibrational frequencies of the gas molecules upon complex formation with various CNS have also been computed. Significant changes in the polarizability values have been observed for the carbon materials on binding with the gas molecules, which can be further monitored to detect the presence of the analyte for sensor applications. It has also been found that the HOMO–LUMO energy gap of the CNS remains unaffected by the binding of these gas molecules. We hope that our results would be helpful to develop novel carbon material-based sensors.

## Supporting information available

Polarizability, HOMO energy and LUMO energy values of various CNSs, Mulliken charge of the molecules at M06-2X/6-311G\*\*//ONIOM(M06-2X/6-31G\*: AM1) level of theory and HOMO–LUMO energy gap of CNS before and after complex formation with the small molecules M06-2X/6-311G\*\* level.

1. Dinadayalane, T. C. and Leszczynski, J., Remarkable diversity of carbon–carbon bonds: structures and properties of fullerenes, carbon nanotubes, and graphene. *Struct. Chem.*, 2010, **21**, 1155–1169.
2. Liang, F. and Chen, B., A review on biomedical applications of single-walled carbon nanotubes. *Curr. Med. Chem.*, 2010, **17**, 10–24.

3. Zhu, Y., Murali, S., Cai, W., Li, X., Suk, J. W., Potts, J. R. and Ruoff, R. S., Graphene and graphene oxide: synthesis, properties, and applications. *Adv. Mater.*, 2010, **22**, 3906–3924.
4. Goldoni, A., Larciprete, R., Petaccia, L. and Lizzit, S., Single-wall carbon nanotube interaction with gases: sample contaminants and environmental monitoring. *J. Am. Chem. Soc.*, 2003, **125**, 11329–11333.
5. Guo, Z. *et al.*, CO<sub>2</sub>-responsive 'smart' single-walled carbon nanotubes. *Adv. Mater.*, 2012, **25**, 584–590.
6. Zhong, J. *et al.*, Interfacial interaction of gas molecules and single-walled carbon nanotubes. *Appl. Phys. Lett.*, 2012, **100**, 201605.
7. Star, A., Joshi, V., Skarupo, S., Thomas, D. and Gabriel, J. P., Gas sensor array based on metal-decorated carbon nanotubes. *J. Phys. Chem. B*, 2006, **110**, 21014–21020.
8. Huang, B. *et al.*, Adsorption of gas molecules on graphene nanoribbons and its implication for nanoscale molecule sensor. *J. Phys. Chem. C*, 2008, **112**, 13442–13446.
9. Wang, F., Gu, H. and Swager, T. M., Carbon nanotube/polythiophene chemiresistive sensors for chemical warfare agents. *J. Am. Chem. Soc.*, 2008, **130**, 5392–5393.
10. Hussain, M. A., Soujanya, Y. and Sastry, G. N., Evaluating the efficacy of amino acids as CO<sub>2</sub> capturing agents: a first principles investigation. *Environ. Sci. Technol.*, 2011, **45**, 8582–8588.
11. Srivastava, H. K. and Sastry, G. N., Viability of clathrate hydrates as CO<sub>2</sub> capturing agents: a theoretical study. *J. Phys. Chem. A*, 2011, **115**, 7633–7637.
12. Lu, G., Ocola, L. E. and Chen, J., Gas detection using low-temperature reduced graphene oxide sheets. *Appl. Phys. Lett.*, 2009, **94**, 083111.
13. Lu, G., Park, S., Yu, K., Ruoff, R. S., Ocola, L. E., Rosenmann, D. and Chen, J., Toward practical gas sensing with highly reduced graphene oxide: a new signal processing method to circumvent run-to-run and device-to-device variations. *ACS Nano*, 2011, **5**, 1154–1164.
14. Lu, G., Yu, K., Ocola, L. E. and Chen, J., Ultrafast room temperature NH<sub>3</sub> sensing with positively gated reduced graphene oxide field-effect transistors. *Chem. Commun.*, 2011, **47**, 7761–7763.
15. Jacobs, C. B., Peairs, M. J. and Venton, B. J., Carbon nanotube based electrochemical sensors for biomolecules. *Anal. Chim. Acta*, 2010, **662**, 105–127.
16. Kong, J., Franklin, N., Zhou, C., Chapline, M., Peng, S., Cho, K. and Dai, H., Nanotube molecular wires as chemical sensors. *Science*, 2000, **287**, 622–625.
17. Schedin, F., Geim, A. K., Morozov, S. V., Hill, E. W., Blake, P., Katsnelson, M. I. and Novoselov, K. S., Detection of individual gas molecules adsorbed on graphene. *Nature Mater.*, 2007, **6**, 652–655.
18. Umadevi, D. and Sastry, G. N., Molecular and ionic interaction with graphene nanoflakes: a computational investigation of CO<sub>2</sub>, H<sub>2</sub>O, Li, Mg, Li<sup>+</sup>, and Mg<sup>2+</sup> interaction with polycyclic aromatic hydrocarbons. *J. Phys. Chem. C*, 2011, **115**, 9656–9667.
19. Umadevi, D. and Sastry, G. N., Metal ion binding with carbon nanotubes and graphene: effect of chirality and curvature. *Chem. Phys. Lett.*, 2012, **549**, 39–43.
20. Ravinder, P., Kumar, R. M. and Subramanian, V., Studies on the encapsulation of F<sup>-</sup> in single walled nanotubes of different chiralities using density functional theory calculations and car-Parrinello molecular dynamics simulations. *J. Phys. Chem. A*, 2012, **116**, 5519–5528.
21. Ghosh, A., Subrahmanyam, K. S., Krishna, K. S., Datta, S., Govindaraj, A., Pati, S. K. and Rao, C. N. R., Uptake of H<sub>2</sub> and CO<sub>2</sub> by graphene. *J. Phys. Chem. C*, 2008, **112**, 15704–15707.
22. Srinivasu, K., Chandrakumar, K. R. S. and Ghosh, S. K., Quantum chemical studies on hydrogen adsorption in carbon-based model systems: role of charged surface and the electronic induction effect. *Phys. Chem. Chem. Phys.*, 2008, **10**, 5832–5839.
23. Nagaraju, M. and Sastry, G. N., Theoretical studies on inclusion complexes of cyclodextrins. *J. Phys. Chem. A*, 2009, **113**, 9533–9542.
24. Derouane, E. G., The energetics of sorption by molecular sieves: surface curvature effects. *Chem. Phys. Lett.*, 1987, **142**, 200–204.
25. Derouane, E. G., Andre, J.-M. and Lucas, A. A., Surface curvature effects in physisorption and catalysis by microporous solids and molecular sieves. *J. Catal.*, 1988, **110**, 58–73.
26. Derycke, I., Vigneron, J. P., Lambin, Ph., Lucas, A. A. and Derouane, E. G., Physisorption in confined geometry. *J. Chem. Phys.*, 1991, **94**, 4620–4627.
27. Chopra, S., McGuire, K., Gothard, N. and Rao, A. M., Selective gas detection using a carbon nanotube sensor. *Appl. Phys. Lett.*, 2003, **83**, 2280–2282.
28. Li, J., Lu, Y., Ye, Q., Cinke, M., Han, J. and Meyyappan, M., Carbon nanotube sensors for gas and organic vapor detection. *Nano Lett.*, 2003, **3**, 929–933.
29. Mirica, K. A., Weis, J. G., Schnorr, J. M., Esser, B. and Swager, T. M., Mechanical drawing of gas sensors on paper. *Angew. Chem., Int. Ed. Engl.*, 2012, **51**, 10740–10745.
30. Yu, K., Lu, G., Bo, Z., Mao, S. and Chen, J., Carbon nanotube with chemically bonded graphene leaves for electronic and optoelectronic applications. *J. Phys. Chem. Lett.*, 2011, **2**, 1556–1562.
31. Yu, K., Wang, P., Lu, G., Chen, K., Bo, Z. and Chen, J., Patterning vertically oriented graphene sheets for nanodevice applications. *J. Phys. Chem. Lett.*, 2011, **2**, 537–542.
32. Britz, D. A. and Khlobystov, A. N., Noncovalent interactions of molecules with single walled carbon nanotubes. *Chem. Soc. Rev.*, 2006, **35**, 637–659.
33. Wang, C., Li, S., Zhang, R. and Lin, Z., Adsorption and properties of aromatic amino acids on single-walled carbon nanotubes. *Nanoscale*, 2012, **4**, 1146–1153.
34. Zhang, Z., Huang, H., Yang, X. and Zang, L., Tailoring electronic properties of graphene by  $\pi$ - $\pi$  stacking with aromatic molecules. *J. Phys. Chem. Lett.*, 2011, **2**, 2897–2905.
35. Das, A., Sood, A. K., Maiti, P. K., Das, M., Varadarajan, R. and Rao, C. N. R., Binding of nucleobases with single-walled carbon nanotubes: theory and experiment. *Chem. Phys. Lett.*, 2008, **453**, 266–273.
36. Kar, T., Bettinger, H. F., Scheiner, S. and Roy, A. K., Noncovalent  $\pi$ - $\pi$  Stacking and CH... $\pi$  interactions of aromatics on the surface of single-wall carbon nanotubes: an MP2 study. *J. Phys. Chem. C*, 2008, **112**, 20070–20075.
37. Vijay, D. and Sastry, G. N., Exploring the size dependence of cyclic and acyclic  $\pi$ -systems on cation- $\pi$  binding. *Phys. Chem. Chem. Phys.*, 2008, **10**, 582–590.
38. Priyakumar, U. D. and Sastry, G. N., Cation- $\pi$  interactions of curved polycyclic systems: M<sup>+</sup> (M = Li and Na) ion complexation with buckybowls. *Tetrahedron Lett.*, 2003, **44**, 6043–6046.
39. Priyakumar, U. D., Punnagai, M., Krishna Mohan, G. P. and Sastry, G. N., A computational study of cation- $\pi$  interactions in polycyclic systems: exploring the dependence on the curvature and electronic factors. *Tetrahedron*, 2004, **60**, 3037–3043.
40. Mahadevi, A. S. and Sastry, G. N., Cation- $\pi$  Interaction: its role and relevance in chemistry, biology, and material science. *Chem. Rev.*, 2013, **113**, 2100–2138.
41. Chourasia, M., Sastry, G. M. and Sastry, G. N., Aromatic-aromatic interactions database, A<sup>2</sup>ID: an analysis of aromatic  $\pi$ -networks in proteins. *Int. J. Biol. Macromol.*, 2011, **48**, 540–552.
42. Rao, C. N. R., Sood, A. K., Subrahmanyam, K. S. and Govindaraj, A., Graphene: the new two-dimensional nanomaterials. *Angew. Chem., Int. Ed. Engl.*, 2009, **48**, 7752–7777.
43. Umadevi, D. and Sastry, G. N., Quantum mechanical study of physisorption of nucleobases on carbon materials: graphene versus carbon nanotubes. *J. Phys. Chem. Lett.*, 2011, **2**, 1572–1576.

44. Umadevi, D. and Sastry, G. N., Impact of the chirality and curvature of carbon nanostructures on their interaction with aromatics and amino acids. *ChemPhysChem*, 2013, **14**, 2570–2578.
45. Balamurugan, K., Singam, E. R. A. and Subramanian, V., Effect of curvature on the  $\alpha$ -helix breaking tendency of carbon based nanomaterials. *J. Phys. Chem. C*, 2011, **115**, 8886–8892.
46. Chandrakumar, K. R. S., Srinivasu, K. and Ghosh, S. K., Nano-scale curvature-induced hydrogen adsorption in alkali metal doped carbon nanomaterials. *J. Phys. Chem. C*, 2008, **112**, 15670–15679.
47. Zuo, G., Zhou, X., Huang, Q., Fang, H. and Zhou, R., Adsorption of villin headpiece onto graphene, carbon nanotube, and C60: effect of contacting surface curvatures on binding affinity. *J. Phys. Chem. C*, 2011, **115**, 23323–23328.
48. Charlier, J. C., Defects in carbon nanotubes. *Acc. Chem. Res.*, 2002, **35**, 1063–1069.
49. Chen, R. J. *et al.*, Noncovalent functionalization of carbon nanotubes for highly specific electronic biosensors. *Proc. Natl. Acad. Sci. USA*, 2003, **100**, 4984–4989.
50. Cazorla, C., Shevlin, S. A. and Guo, Z. X., Calcium-based functionalization of carbon materials for CO<sub>2</sub> capture: a first-principles computational study. *J. Phys. Chem. C*, 2011, **115**, 10990–10995.
51. Georgakilas, V. *et al.*, Functionalization of graphene: covalent and non-covalent approaches, derivatives and applications. *Chem. Rev.*, 2012, **112**, 6156–6214.
52. Beheshtian, J., Baei, M. T., Bagheri, Z. and Peyghan, A. A., Carbon nitride nanotube as a sensor for alkali and alkaline earth cations. *Appl. Surf. Sci.*, 2013, **264**, 699–706.
53. Wang, X. and Liew, K. M., Silicon carbide nanotubes serving as a highly sensitive gas chemical sensor for formaldehyde. *J. Phys. Chem. C*, 2011, **115**, 10388–10393.
54. Zhao, Y. and Truhlar, D. G., The M06 suite of density functionals for main group thermochemistry, thermochemical kinetics, noncovalent interactions, excited states, and transition elements: two new functionals and systematic testing of four M06-class functionals and 12 other functionals. *Theor. Chem. Acc.*, 2008, **120**, 215–241.
55. Mahadevi, A. S., Neela, Y. I. and Sastry, G. N., A theoretical study on structural, spectroscopic and energetic properties of acetamide clusters [CH<sub>3</sub>CONH<sub>2</sub>] ( $n = 1-15$ ). *Phys. Chem. Chem. Phys.*, 2011, **13**, 15211–15220.
56. Vijay, D. and Sastry, G. N., The impact of basis set superposition error on the structure of  $\pi$ - $\pi$  dimers. *Int. J. Quantum Chem.*, 2011, **111**, 1893–1901.
57. Neela, Y. I., Mahadevi, A. S. and Sastry, G. N., Hydrogen bonding in water clusters and their ionized counterparts. *J. Phys. Chem. B*, 2010, **114**, 17162–17171.
58. Zhao, Y., Tishchenko, O. and Truhlar, D. G., How well can density functional methods describe hydrogen bonds to  $\pi$  acceptors? *J. Phys. Chem. B*, 2005, **109**, 19046–19051.
59. Denis, P. A., Theoretical investigation of the stacking interactions between curved conjugated systems and their interaction with fullerenes. *Chem. Phys. Lett.*, 2011, **516**, 82–87.
60. Frisch, M. J. *et al.*, Gaussian 09, Revision C.01, Gaussian, Inc., Wallingford, CT, USA, 2010.

ACKNOWLEDGEMENTS. D.U. thanks CSIR, New Delhi for financial assistance. We thank DST, New Delhi and CSIR for funding in the form of 12th five-year projects INTELCOAT.